参赛队员姓名：黄飞扬

中学：深圳中学

省份：广东省

国家/地区：中国

指导教师姓名：汪正平，么依民

论文题目：Facile Fabrication of Silicon Carbide Spheres and Its Application in Polymer Composites with Enhanced Thermal Conductivity

ABSTRACT

Nowadays, as electronic devises thrive, there is an urgent requirement of satisfactory thermal management materials to help efficiently diffuse the accumulated heat in modern electronics. The high-loading addition of thermally conductive filler into polymer is able to significantly enhance the thermal conductivity, but it will inevitably cause serious degradation of mechanical properties. Thus, how to achieve desired thermal conductivity at relatively low filler content still maintains challenging. In this study, a facile strategy to fabricate silicon carbide spheres (SiCSs) is reported, which can be applied as efficient fillers to construct three-dimensional (3D) filler skeleton in the polymer matrix. The obtained silicon carbide spheres exhibit fancy sea urchin-like microstructure with an obvious radiating pattern. The polymer composites were finally prepared by adding the SiCSs into epoxy resin matrix. A satisfactory thermal conductivity of 0.91 $Wm^{-1}K^{-1}$ with the addition of 4.6 vol% SiCSs was achieved in the obtained composites. Moreover, the final thermal conductivity can be easily regulated by varying the added number of SiCSs. The above results illustrate that the SiCSs/epoxy composites exhibit high potential for application in thermal management field.

KEYWORDS: Sphere, Ice-templated assembly, Thermal conductivity, Polymer composite, Silicon carbide

1. INTRODUCTION

Modern electronics nowadays require higher performance, and the heat accumulation caused by high density of integration and power can seriously affect the working efficiency and lifetime of electronic devices [1-4]. In electronic devices, thermal management material

acts as heat conduction paths to transfer the heat from the inside chip to the outside hot sink, where its intrinsic thermal conductivity and mechanical property make a great difference in the thermal management of electronics [5-8]. Polymers are commonly used as the constituting matrix in thermal management materials because of their excellent properties such as low processing temperature, low density, and low cost. However, traditional polymers exhibit rather low TC value (～0.2 $Wm^{-1}K^{-1}$) because of disorderly assembled polymer chains. Therefore, it is necessary to add highly thermally conductive fillers into polymer matrix to improve the heat transferring ability [9]. There are two problems to be solved in the previous researches. The first one is that taking no account of other properties such as mechanical and dielectrical property, the most straightforward strategy to achieve satisfied thermal transferring performance is to add thermally conductive fillers to the greatest extent to construct thermal skeleton inside the polymer matrix. However, the high filler loading would not only bring serious reduction of mechanical property of the polymer matrix, but also results in higher cost; (2) The thermal conductivity of the resultant polymer composites was not enhanced ideally. The use of nano-scale fillers with high specific area introduces more filler/polymer interfaces. The increased interfaces will lead to the reduction of thermal conductivity. Therefore, using fillers with larger dimensions to achieve wanted value of thermal conductivity under low percolation threshold is still challenging.

To overcome these limitations, pre-building three-dimensional (3D) filler skeleton inside the polymer matrix is the keynote of recent studies [5, 9-15]. Well-aligned filler skeleton that overcomes the percolation threshold is able to reduce the interfacial thermal resistance *via* decreasing the number of interfaces, and improve the heat conducting efficiency. We have

devised several kinds of 3D filler skeleton on the basic of ice-templated assembly process. For example, applying boron nitride plates and silicon carbide wire as basic assembly unit, we successfully prepared a 3D hybrid skeleton. Ice-templated assembly along with sintering at 900°C was applied to introduce aligned and solid thermal pathways. The high-temperature sintering is able to introduce borosilicate glass phase at the interface where the newly formed interfacial junctions could act as bridges for phonon transporting. The prepared hybrid boron nitride-silicon carbide skeleton exhibits satisfactory enhancement efficiency of thermal conductivity. With the addition of 8.35 vol% of the hybrid skeleton, the resultant polydimethylsiloxane composites exhibit a desired thermal conductivity as high as 3.87 $Wm^{-1}K^{-1}$. This thought could achieve satisfactory enhancement of thermal conductivity. However, this method is limited by relatively complicated fabrication process. In addition, the boundary dimension of the 3D skeleton is restricted to the mold, which is unfavorable for large-scale production.

In this study, we introduce the facile fabrication of 3D silicon carbide spheres (SiCSs). The SiCSs can be straightly prepared by adding the SiC-contained dispersion into liquid nitrogen after several seconds of assembly process. As a result, the obtained SiCSs exhibit hierarchical 3D microstructure with radial alignments. SiCSs were then introduced into epoxy resin as fillers. Since the SiCSs themselves are part of the macroscopic thermal skeleton, the final thermal conductivity of SiCSs/epoxy composites could be easily controlled by adjusting the number of the added SiCSs. With the addition of 4.6 vol% SiCSs (～40 number of SiCSs), the thermal conductivity of the obtained polymer composites can reach 0.91 $Wm^{-1}K^{-1}$. Moreover, this method is not limited to the fixed shape of the mold as the addition of SiCSs is

easier for operation. These results illustrate that the strategy to fabricate SiCSs along with the corresponding SiCSs/epoxy composites could serve as high-performance thermal management.

2. EXPERIMENTAL SECTION

2.2 Fabrication of spherical silicon carbide aerogels and their composites.

A certain amount of silicon carbide nanowires and sodium carboxymethyl cellulose was added into deionized water, followed by sonication for 60 min to generate a uniform SiC-contained dispersion. The SiCSs were prepared by adding the SiC-contained dispersion slowly into liquid nitrogen. The frozen SiCSs were finally collected by removing the resident liquid nitrogen from the container and put into freeze-drier for removing the ice crystals. Before adding into epoxy resin, the SiCSs were sintered at 900°C for 10 hours. The SiCSs/epoxy composites were fabricated by adding SiCSs into epoxy resin by the help of vacuum-assisted infiltration. The composites were then thermally cured at several temperature.

3. RESULTS AND DISCUSSION

3.1 Preparation of SiCSs

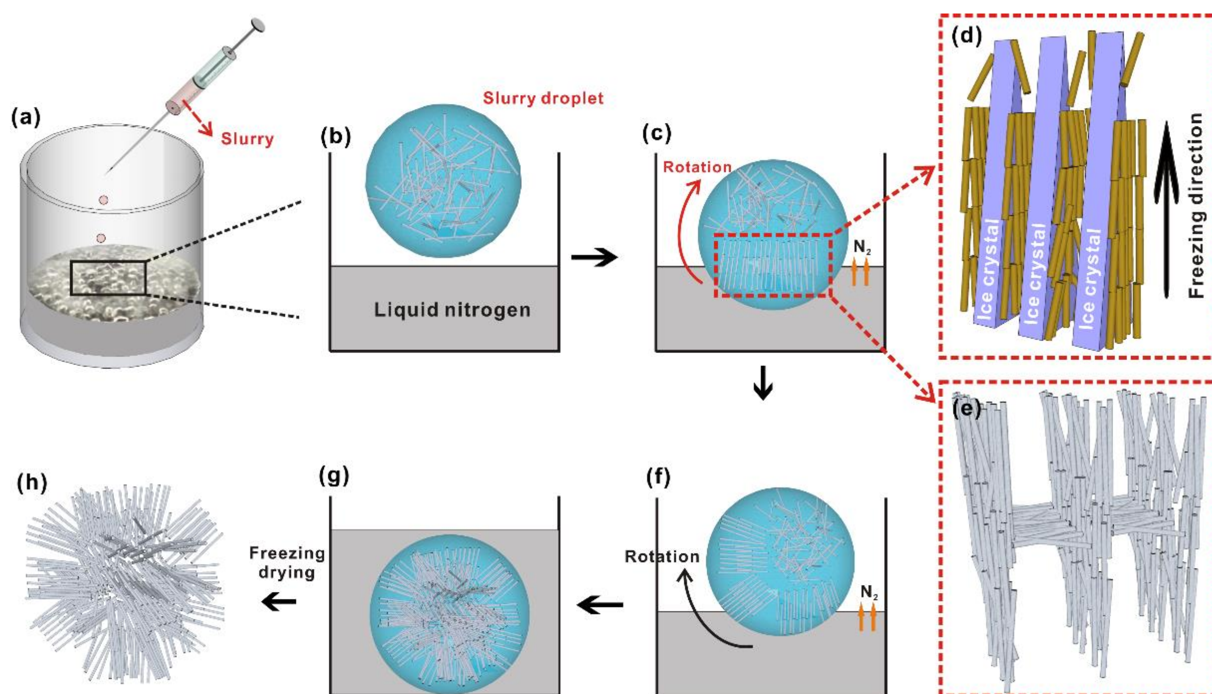

Figure 1. Schematic illustration of the fabrication process of SiCSs.

The SiCSs were prepared *via* two consecutive and repetitive assembly process. The one is ice-templated assembly or so-called freeze casting in local area. The other one is the volatilization of liquid nitrogen-driven rotation on the surface of liquid nitrogen. The formation of SiCSs is the comprehensive result of these two assembly processes. Figure 1 shows the typical preparation process of SiCSs. Firstly, the SiC aqueous dispersion that contain nanowires was added into liquid nitrogen by a syringe (Figure 1a, b). As the dispersion drop moved close to the surface of liquid nitrogen, the intrinsic low temperature (-196 °C) of liquid nitrogen instantaneously produced a huge temperature gradient, leading to local ice-templated assembly (Figure 1c). In the dispersion, SiC nanowires were squeezed by the varying ice crystals along the temperature gradient and piled up into SiC aggregates (Figure 1d). The ice-templated assembly occurred in local area leads to the formation of well-aligned channels along the through-plane direction (Figure 1e). As the local

ice-templated assembly was done, the steady state would be destroyed due to the density variation caused by the volume expansion during the liquid-solid phase transition. The unfrozen part would move close to the surface of liquid nitrogen and repeat the mentioned procedures (Figure 1f). When the liquid-solid phase transition was fully achieved in the dispersion, the dispersion drop would sink into the liquid nitrogen (Figure 1g). The SiCSs were finally obtained by freeze-drying the frozen slurry droplets (Figure 1h), followed by high-temperature sintering.

3.2 Structurally Characterization of SiCSs

Figure 2 exhibits the microstructure of the obtained SiCSs. The aspect ratio of SiC nanowires was estimated to be in the range of 120-160 (Figure 2a). The SiCSs show a diameter of 2.5 mm (Figure 2b) with lots of oriented, intricate and long-range channels as appearance. Certain number of macroscopic pores also exist on the surface (Figure 2c). Figure 2d-f exhibits highly interconnected pores with obvious aligned SiC layers. The axial skeleton was mainly the result of ice-templated assembly. Meanwhile, the radial skeleton was formed *via* the balance between the growth of ice crystals and the viscosity of the system. Higher viscosity would hinder SiC nanowires from freely moving upon the repulsion of the growing ice crystals during the assembly. The ice crystals might be fixed as the SiC nanowires have not been able to arrange parallel to them, forming horizontal SiC bridges perpendicularly to the SiC layers.

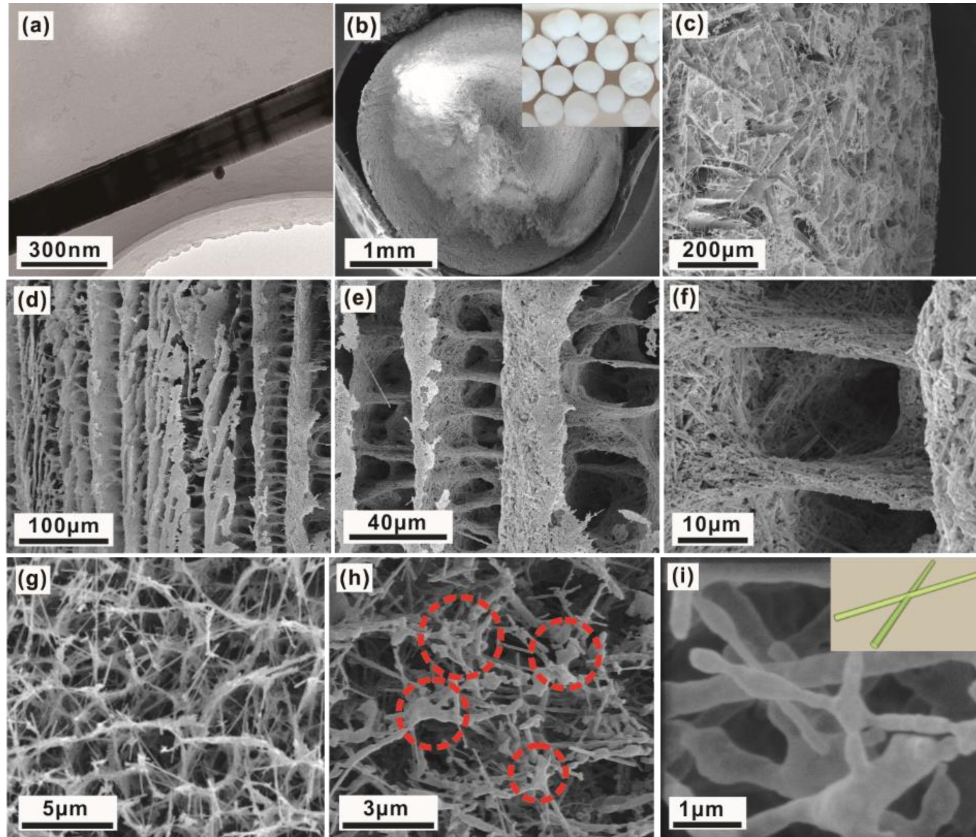

Figure 2. Structural characterization of SiCSs. (a) SEM image of a single slice of SiC nanowire; (b) SEM and digital images of SiCSs; (c-g) surface morphology of SiCSs at different magnifications; (h, i) SEM images of SiC-SiC junction at different dimensions.

The representative morphology of SiC-SiC junction after sintering at 900 °C was shown in Figure 2g-i, where the resident SiC liquid phase can still be detected. High temperature would accelerate the atom movement at the junction interface and facilitate the formation of junction bonding at SiC/SiC interface. The sintering-introduced interface adhesion is much stronger than Van der Waals force or hydrogen bond due to the atom-level interconnection. This is beneficial for further reduce the interfacial thermal resistance.

3.3 Characterization of SiCSs/Epoxy Composites

Figure 3a shows a digital image of SiCSs/epoxy composites where SiCSs could be clearly seen. The surface morphology of the sample indicates the pores within the SiCSs are fully filled with epoxy resin. The cross-sectional morphology was characterized as shown in Figure 3b, c. There are no gaps between SiC layers and cured epoxy resin, indicating the interfacial adhesion between SiC and epoxy is relatively strong. SiC skeleton is well maintained as shown in Figure 3b and c, indicating SiC layer could serve as aligned thermal pathways. The through-plane skeleton could provide expressways for phonon transport, thus enhancing the thermal conducting performance. Elemental distribution scanning was further used to confirm the dispersion state of SiC skeleton in epoxy matrix, as shown in Figure 3d, e. The spectrogram of element Si further confirms that the SiC skeleton maintains its origin orientation. On the other hand, the spectrogram of element C further confirms the epoxy resin is uniformly filled in the gaps between adjacent SiC layers. The perpendicular SiC bridges are not that obvious as they might be fully encapsulated by epoxy resin due to smaller dimensions.

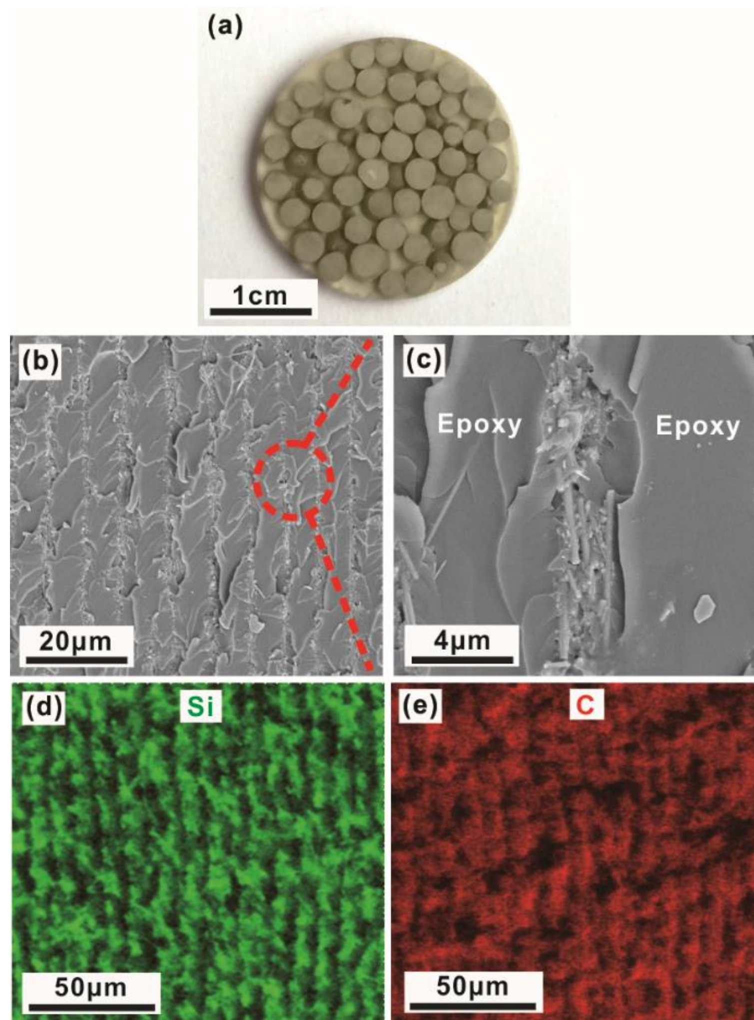

Figure 3. Morphologic characterization of SiCSs/epoxy composites. (a) Digital image of SiCSs/epoxy composite. (b, c) Cross-sectional morphology of SiCSs/epoxy composite at different magnifications. Elemental distribution spectrogram of elements Si (d) and C (e), respectively.

3.4 Thermal Characterization of SiCSs/Epoxy Composites

Epoxy composite filled with Al_2O_3, AlN and SiC particles at the same volume loading were also separately prepared to illustrate the advantage of SiCSs, as shown in Figure 4a. In Figure 4b, pure epoxy resin possesses a low intrinsic thermal conductivity of 0.19 $Wm^{-1}K^{-1}$, which falls in the similar range with previous studies [3]. At the same filler loading (4.6 vol%), the

SiCSs/epoxy composite demonstrates the best thermal conducting performance with a thermal conductivity of 0.91 $Wm^{-1}K^{-1}$ when compared to epoxy composites with Al_2O_3, AlN and SiC particles, suggesting the advantage of the unique structure of SiCSs. Since the SiCSs themselves are the basic unit of the macroscopic thermal skeleton in the epoxy matrix, the resultant thermal conductivity could be easily manipulated by the added number of SiCSs.

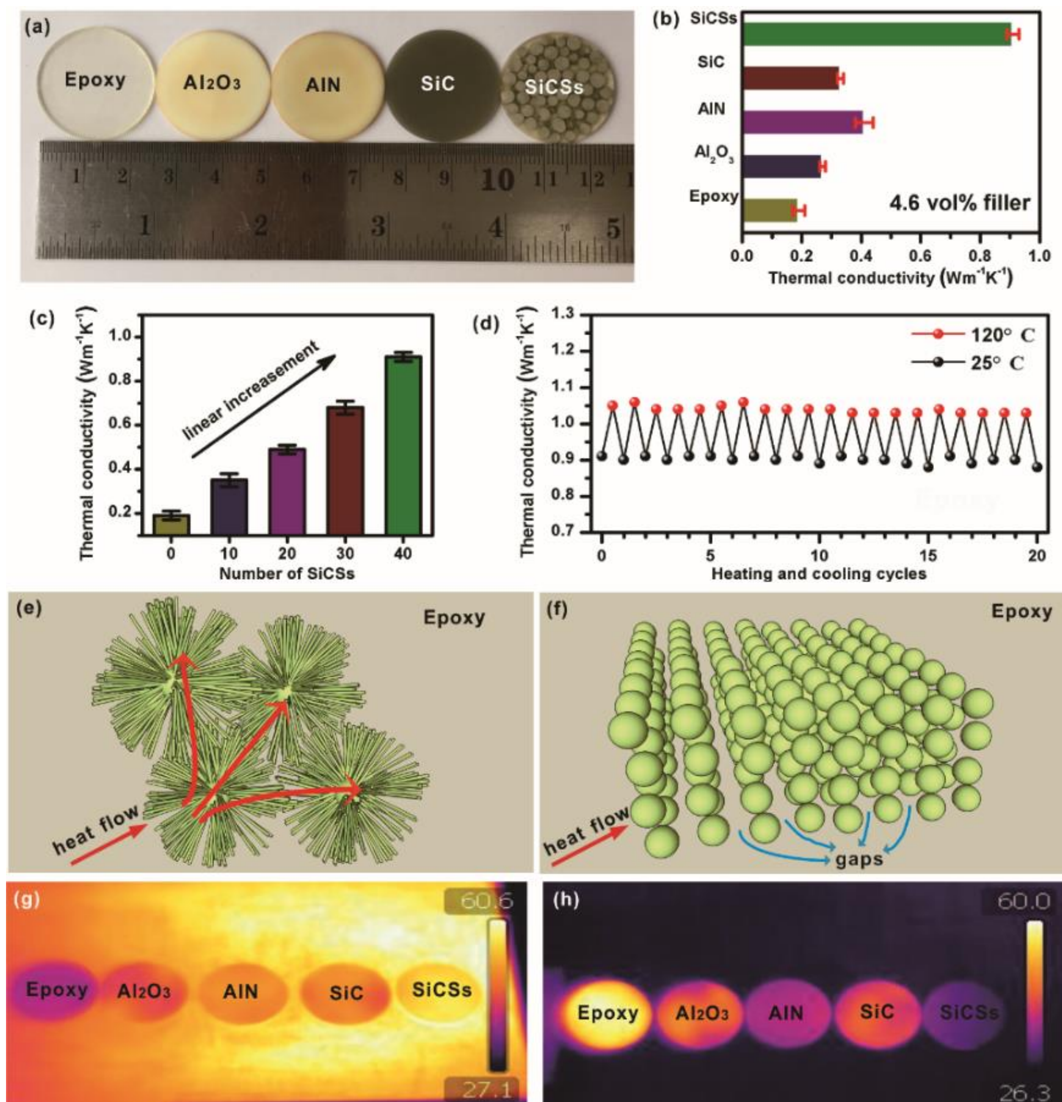

Figure 4. Thermal conductivity of the SiCSs/epoxy composites. (a) Digital images of epoxy matrix, epoxy composites filled with Al_2O_3, AlN, SiC particles and SiCSs, respectively; (b) Corresponding values of thermal conductivity of the samples as shown in (a);

(c) Thermal conductivity of SiCSs/epoxy composite with different numbers of SiCSs; (d) Thermal conductivity of a SiCSs/epoxy composite over 20 heating/cooling cycles; Thermal conduction model for (e) SiCSs and (f) SiC nanoparticles; (g, h) Thermal infrared images of SiCSs/epoxy composite and contrastive samples during heating and cooling processes.

As shown in Figure 4c, the thermal conductivity increased from 0.35 $Wm^{-1}K^{-1}$ at 10 number of SiCSs to 0.91 $Wm^{-1}K^{-1}$ at 40 number of SiCSs. The stability of thermal conductivity under repetitive temperature circle is another important parameter to evaluate the comprehensive performance of the composites. The SiCSs/epoxy composites were put in the environment of 25 and 120 °C, respectively, while the variations of thermal conductivity were recorded in Figure 4d. The thermal conductivity basically maintained its origin value of thermal conductivity at 25 and 120 °C, respectively, showing good stability of thermal conductivity during this temperature range. The integration of high porosity with the ice-templated microstructure of SiCSs contribute to the formation of thermally conductive network at low filler loading, as shown in Figure 4e. In contrast to SiCSs, randomly-dispersed filler particles in epoxy resin could hardly form thermal network due to the gaps as shown in Figure 4f, and thus decreasing the thermal conductivity. To demonstrate the practical feasibility of SiCSs/epoxy composites, the sample was put on a metal plate to see the temperature variation during heating and cooling process, respectively. SiCSs/epoxy and other three comparative samples (Al_2O_3, AlN and SiC) were then put on the same metal plate under the same heating environment where the surface temperature was recorded by an infrared thermal imager. As shown in Figure 4g, the temperature of SiCSs/epoxy composite exhibits much faster increase in comparison with other samples during the heat absorption

process, indicating that it has better thermal response originating from high intrinsic thermal conductivity. On the other hand, the temperature of SiCSs/epoxy composite decreases faster than other three comparative samples, as is exhibited in Figure 4h The above results demonstrate SiCSs/epoxy composites are able to efficiently diffuse the generated heat and act as high-performance thermal management materials.

3.4 Thermal Simulation of SiCSs/Epoxy Composites *via* COMSOL

We carried out a 2D finite element simulation with COMSOL MULTIPHYSICS for comparing the heat conduction between the silicon carbide nanowire spheres with the normal silicon carbide spheres. The diameter and the length of the silicon carbide nanowire are 0.2um and 10um. Considering the equivalent volume, the normal silicon carbide sphere has a diameter of 6.32um. The silicon carbide spheres are immersed in an epoxy resin with a width of 40um and a height of 24um, as shown in Figure 5. The thermal conductivity of silicon carbide is 80 W/(mK), and the thermal conductivity of epoxy resin is 0.17 W/(mK).

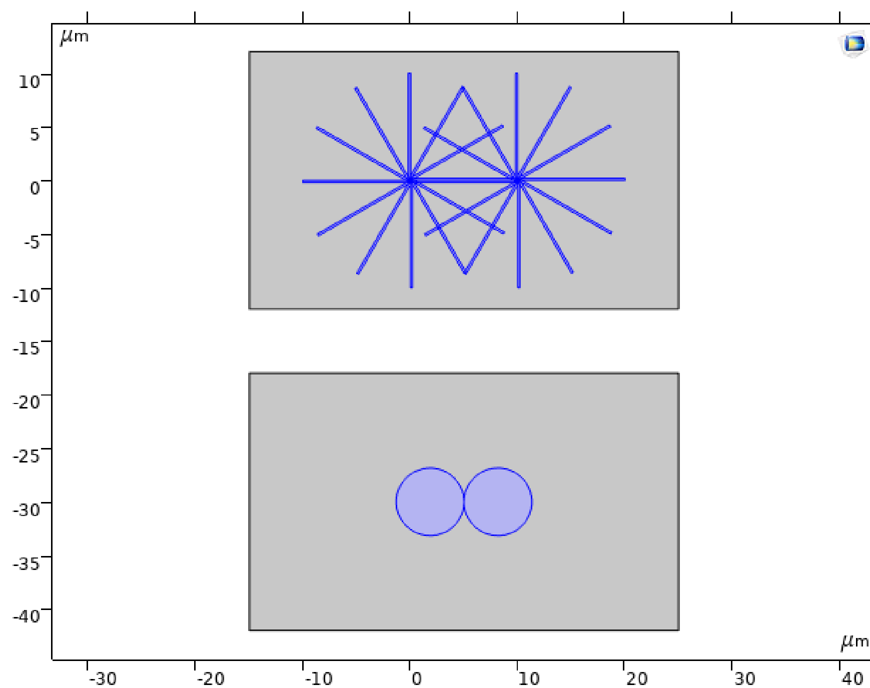

Figure 5. COMSOL model of epoxy composites filled with SiCSs and SiC particles, respectively.

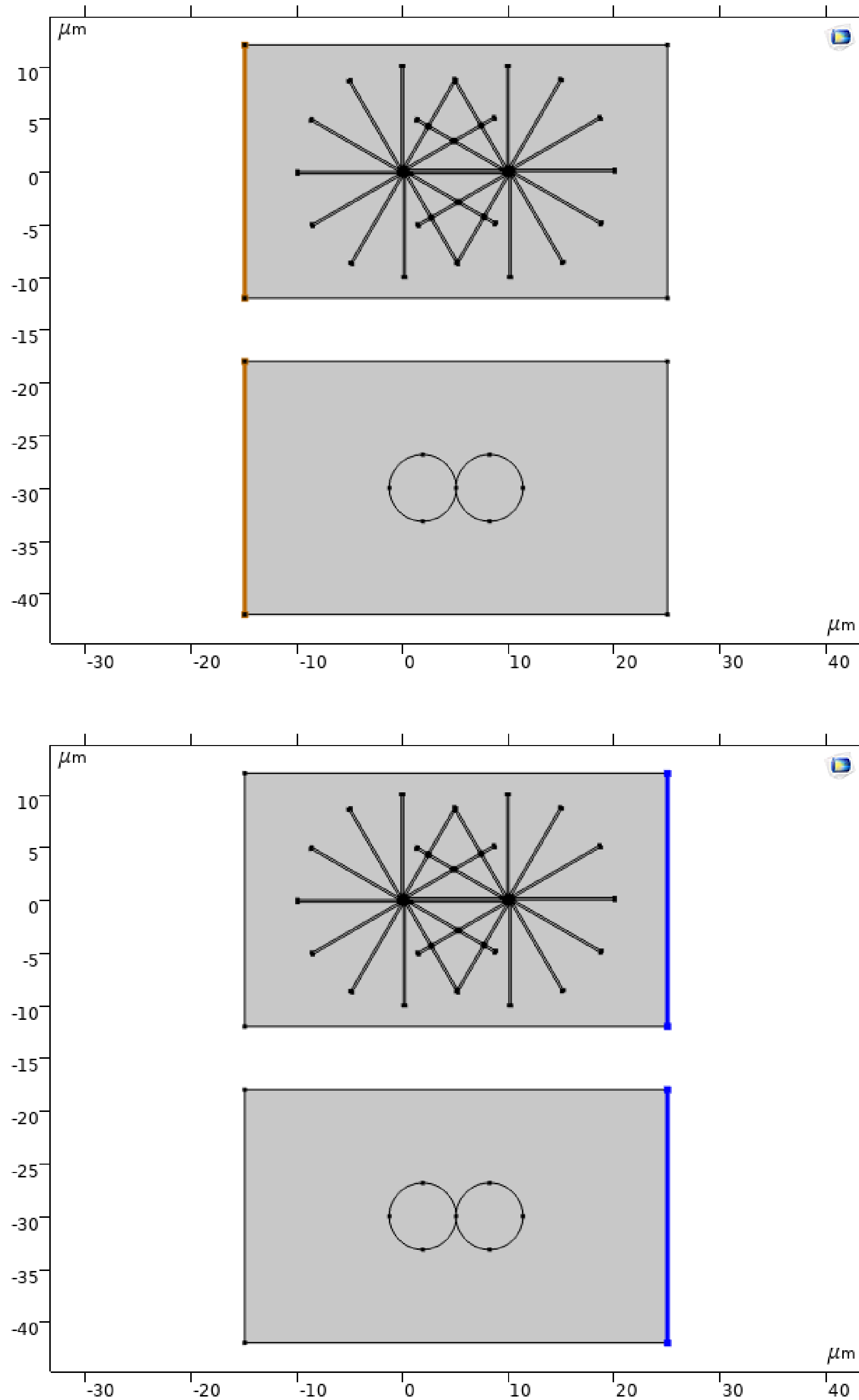

Figure 6. The demonstration of heat flux through the epoxy composites.

We set a fixed inward heat flux at the left side of the epoxy resin as q0=200000W/m^2 as is shown in Figure 6. and a fixed temperature as 300K at the right side. The rest parts of the boundaries are set as thermal insulation.

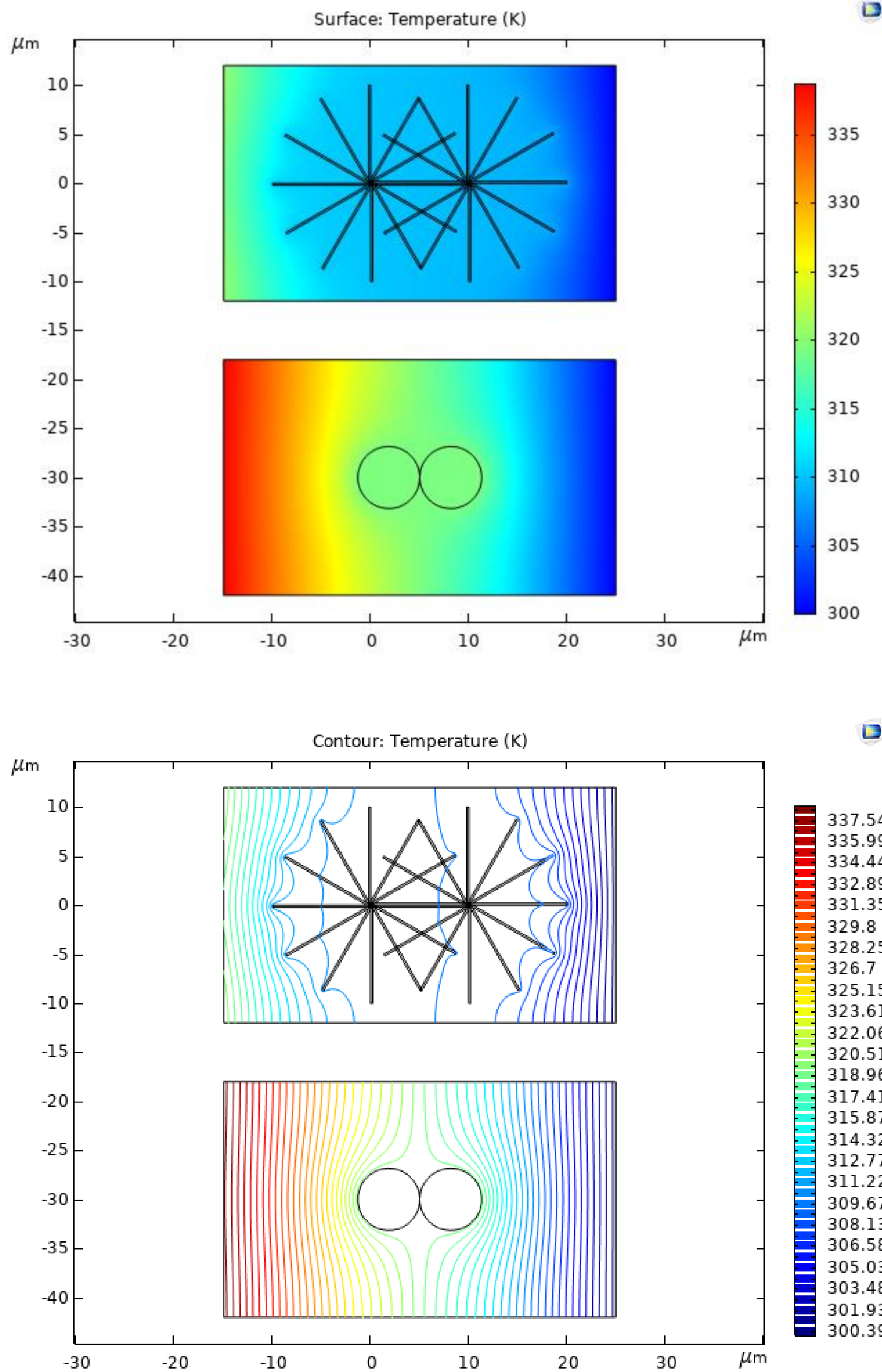

Figure 7. The demonstration of heat flux through the epoxy composites.

The simulation result in Figure 7 shows that the surface temperature of the silicon carbide nanowire spheres sample is much lower than the normal silicon carbide spheres one, which indicates the silicon carbide nanowire spheres sample has a much better heat conduction ability. The average temperature at the left boundary of the silicon carbide nanowire spheres sample is 319.61K, which is lower than the temperature of 338.59K from the normal one. The equivalent thermal conductivity of the silicon carbide nanowire spheres sample is around 2 times as the normal one.

4. CONCLUSIONS

In conclusion, we have applied a simple strategy to prepare SiCSs on the basic of conventional ice-templated assembly technology. Originating from the local assembly along with the rotation on the surface of liquid nitrogen, the obtained SiCSs possess cyclical, open and throughout pores on the surface with diameter falling in the range of millimeter. The addition of SiCSs contributes to higher enhancing efficiency of thermal conductivity than other commercial fillers. Moreover, the thermal conductivity was easily regulated *via* varying the number of added SiCSs. By employing this unique three-dimensional skeleton, we demonstrate the great potential of SiCSs applied as efficient thermal management materials.

REFERENCES

[1] Derue, L., Dautel, O., Tournebize, A., Drees, M., Pan, H., Berthumeyrie, S., Pavageau, B., Cloutet, E., Chambon, S., Hirsch, L., Rivaton, A., Hudhomme, P., Facchetti, A., and Wantz, G.: 'Thermal Stabilisation of Polymer-Fullerene Bulk Heterojunction Morphology for Efficient Photovoltaic Solar Cells', Adv. Mater., 2014, 26, (33), pp. 5831-5838.

[2] Moore, A.L., and Shi, L.: 'Emerging Challenges and Materials for Thermal Management of Electronics', Mater. Today, 2014, 17, (4), pp. 163-174.

[3] Lian, G., Tuan, C.-C., Li, L., Jiao, S., Wang, Q., Moon, K.-S., Cui, D., and Wong, C.-P.: 'Vertically Aligned and Interconnected Graphene Networks for High Thermal Conductivity of Epoxy Composites with Ultralow Loading', Chem. Mater., 2016, 28, (17), pp. 6096-6104.

[4] Shen, H., Cai, C., Guo, J., Qian, Z., Zhao, N., and Xu, J.: 'Fabrication of Oriented hBN Scaffolds for Thermal management materials', RSC Adv., 2016, 6, (20), pp. 16489-16494.

[5] Fu, L., Wang, T., Yu, J., Dai, W., Sun, H., Liu, Z., Sun, R., Jiang, N., Yu, A., and Lin, C.-T.: 'An Ultrathin High-Performance Heat Spreader Fabricated with Hydroxylated Boron Nitride Nanosheets', 2D Mater., 2017, 4, (2), 025047.

[6] Shen, D., Zhan, Z., Liu, Z., Cao, Y., Zhou, L., Liu, Y., Dai, W., Nishimura, K., Li, C., Lin, C.-T., Jiang, N., and Yu, J.: 'Enhanced Thermal Conductivity of Epoxy Composites Filled with Silicon Carbide Nanowires', Sci. Rep., 2017, 7, 2606.

[7] Lu, H., Zhang, J., Luo, J., Gong, W., Li, C., Li, Q., Zhang, K., Hu, M., and Yao, Y.: 'Enhanced Thermal Conductivity of Free-Standing 3D Hierarchical Carbon Nanotube-Graphene Hybrid Paper', Composites, Part A, 2017, 102, pp. 1-8.

[8] Yu, C., Zhang, J., Li, Z., Tian, W., Wang, L., Luo, J., Li, Q., Fan, X., and Yao, Y.: 'Enhanced Through-Plane Thermal Conductivity of Boron Nitride/Epoxy Composites', Composites, Part A, 2017, 98, pp. 25-31.

[9] Hong, H., Kim, J.U., and Kim, T.-I.: 'Effective Assembly of Nano-Ceramic Materials for High and Anisotropic Thermal Conductivity in a Polymer Composite', Polymers, 2017, 9, (9), 413.

[10] Han, Z., and Fina, A.: 'Thermal Conductivity of Carbon Nanotubes and Their Polymer Nanocomposites: A Review', Prog. Polym. Sci., 2011, 36, (7), pp. 914-944.

[11] Chen, H., Ginzburg, V.V., Yang, J., Yang, Y., Liu, W., Huang, Y., Du, L., and Chen, B.: 'Thermal Conductivity of Polymer-Based Composites: Fundamentals and Applications', Prog. Polym. Sci., 2016, 59, pp. 41-85.

[12] Hussain, A.R.J., Alahyari, A.A., Eastman, S.A., Thibaud-Erkey, C., Johnston, S., and Sobkowicz, M.J.: 'Review of Polymers for Heat Exchanger Applications: Factors Concerning Thermal Conductivity', Appl. Therm. Eng., 2017, 113, pp. 1118-1127.

[13] Guo, C., Zhou, L., and Lv, J.: 'Effects of Expandable Graphite and Modified Ammonium Polyphosphate on the Flame-Retardant and Mechanical Properties of Wood Flour-Polypropylene Composites', Polym. Polym. Compos., 2013, 21, (7), pp. 449-456.

[14] Mirkhalaf, M., and Barthelat, F.: 'Nacre-like Materials Using a Simple Doctor Blading Technique: Fabrication, Testing and Modeling', J. Mech. Behav. Biomed. Mater., 2016, 56, pp. 23-33.

[15] Kim, K., and Kim, J.: 'Magnetic Aligned AlN/Epoxy Composite for Thermal Conductivity Enhancement at Low Filler Content', Composites, Part B, 2016, 93, pp. 67-74.

ACKNOWLEDGMENT

I sincerely thanks my volunteer supervisors Yimin Yao and Ching-ping Wong, whom I met during a program in SIAT three years ago. The choice of the topic was determined after the discussing with Ching-Ping Wong, Rong Sun, Jianbing Xu, Yimin Yao, PeiPei Xin, and Fei Deng, for which I am really grateful. I managed to finish the paper, conducted experiments, and processed data on my own. I am grateful for the generous support provided by Ching-Ping Wong and Yimin Yao who volunteered to instruct my experiment, give specialized equipment training, and give constructive advice to my paper.

Since the paper requires a simulation which I am not familiar with, Xue Bai and Jianbin Xu, the researchers in SIAT, helped conduct the theoretical simulation shown in the thesis and gave test instructions.

汪正平 简历

2000 年	**美国国家工程院院士**
2007 年	Sigma Xi’s Monie Ferst 奖
2008 年	美国制造业工程师协会“电子生产卓越贡献奖”
2012 年	德累斯顿巴克豪森奖
2013 年	**中国工程院外籍院士**

黄飞扬 简历

1，在校学业成绩

平均学分绩点（GPA）深圳中学高二国体年级第一

美国大学入学考试（SAT）深圳中学高二国体年级第一

2，荣誉及活动

深圳中学深中之星，腾讯奖学金获得者（全校 10 人）

CTB（全球华人创新研究大挑战）全国前五（约 1500 支队伍参赛）

中学物理知识应用竞赛国家一等奖（排名前千分之三）

深圳中学公开辩论赛冠军

深圳中学 USIYPT（美国青年物理学家邀请赛）校队队长，获第三名；

深圳中学 Discovery 物理研习社主席

SCOPE 世界高中生联合平台主席

深圳中学学生大使